Research Article | Vol. 25, No. 25 | 11 Dec 2017 | OPTICS EXPRESS 31036
Optics EXPRESS

All-organic electro-optic waveguide modulator comprising SU-8 and nonlinear optical polymer

EDGARS NITISS,* ANDREJS TOKMAKOVS, KASPARS PUDZS, JANIS BUSENBERGS, AND MARTINS RUTKIS

Institute of Solid State Physics, University of Latvia, Kengaraga 8, Riga, LV-1063, Latvia
**edgars.nitiss@cfi.lu.lv*

Abstract: In this paper we describe the principles of operation as well as the fabrication and testing steps of an all-organic waveguide modulator. The modulator comprises an SU-8 core and an electro-optic host-guest polymer cladding. The polymer properties are tuned in order to achieve single mode operation. We used direct-write laser lithography in two steps for the preparation of the devices. The electro-optic coefficient of the polymer is estimated from observing the modulation of the device operated in push-pull mode.

OCIS codes: (130.3120) Integrated optics devices; (130.4110) Modulators.

References and links

1. L. R. Dalton, D. Lao, B. C. Olbricht, S. Benight, D. H. Bale, J. A. Davies, T. Ewy, S. R. Hammond, and P. A. Sullivan, "Theory-inspired development of new nonlinear optical materials and their integration into silicon photonic circuits and devices," Opt. Mater. **32**, 658–668 (2010).
2. S. Koeber, R. Palmer, M. Lauermann, W. Heni, D. L. Elder, D. Korn, M. Woessner, L. Alloatti, S. Koenig, P. C. Schindler, H. Yu, W. Bogaerts, L. R. Dalton, W. Freude, J. Leuthold, and C. Koos, "Femtojoule electro-optic modulation using a silicon–organic hybrid device," Light Sci. Appl. **4**, e255 (2015).
3. C. Hoessbacher, A. Josten, B. Baeuerle, Y. Fedoryshyn, H. Hettrich, Y. Salamin, W. Heni, C. Haffner, C. Kaiser, R. Schmid, D. L. Elder, D. Hillerkuss, M. Möller, L. R. Dalton, and J. Leuthold, "Plasmonic modulator with >170 GHz bandwidth demonstrated at 100 GBd NRZ," Opt. Express **25**, 1762 (2017).
4. W. Heni, Y. Kutuvantavida, C. Haffner, H. Zwickel, C. Kieninger, S. Wolf, M. Lauermann, Y. Fedoryshyn, A. F. Tillack, L. E. Johnson, D. L. Elder, B. H. Robinson, W. Freude, C. Koos, J. Leuthold, and L. R. Dalton, "Silicon–Organic and Plasmonic–Organic Hybrid Photonics," ACS Photonics **4**, 1576–1590 (2017).
5. Y. Shi, W. Lin, D. J. Olson, J. H. Bechtel, H. Zhang, W. H. Steier, C. Zhang, and L. R. Dalton, "Electro-optic polymer modulators with 0.8 V half-wave voltage," Appl. Phys. Lett. **77**, 1–3 (2000).
6. L. Alloatti, D. Korn, R. Palmer, D. Hillerkuss, J. Li, A. Barklund, R. Dinu, J. Wieland, M. Fournier, J. Fedeli, H. Yu, W. Bogaerts, P. Dumon, R. Baets, C. Koos, W. Freude, and J. Leuthold, "42.7 Gbit/s electro-optic modulator in silicon technology," Opt. Express **19**(12), 11841–11851 (2011).
7. W. Heni, C. Haffner, D. L. Elder, A. F. Tillack, Y. Fedoryshyn, R. Cottier, Y. Salamin, C. Hoessbacher, U. Koch, B. Cheng, B. Robinson, L. R. Dalton, and J. Leuthold, "Nonlinearities of organic electro-optic materials in nanoscale slots and implications for the optimum modulator design," Opt. Express **25**, 2627 (2017).
8. R. A. Norwood, C. Derose, Y. Enami, H. Gan, C. Greenlee, R. Himmelhuber, O. Kropachev, C. Loychik, D. Mathine, Y. Merzlyak, M. Fallahi, and N. Peyghambarian, "Hybrid sol-gel electro-optic polymer modulators: Beating the drive voltage/loss tradeoff," J. Nonlinear Opt. Phys. Mater. **16**, 217–230 (2007).
9. B. H. Robinson, L. R. Dalton, A. W. Harper, A. Ren, F. Wang, C. Zhang, G. Todorova, M. Lee, R. Aniszfeld, S. Garner, A. Chen, W. H. Steier, S. Houbrecht, A. Persoons, I. Ledoux, J. Zyss, and A. K. Y. Jen, "The molecular and supramolecular engineering of polymeric electro-optic materials," Chem. Phys. **245**, 35–50 (1999).
10. X. Wang, J. Meng, Y. Yue, J. Sun, X. Sun, F. Wang, and D. Zhang, "Fabrication of single-mode ridge SU-8 waveguides based on inductively coupled plasma etching," Appl. Phys., A Mater. Sci. Process. **113**, 195–200 (2013).
11. M. Balakrishnan, M. Faccini, M. B. J. Diemeer, W. Verboom, A. Driessen, D. N. Reinhoudt, and A. Leinse, "Photodefinable electro-optic polymer for high-speed modulators," Electron. Lett. **42**, 51 (2006).
12. M. Balakrishnan, M. Faccini, M. B. J. Diemeer, E. J. Klein, G. Sengo, A. Driessen, W. Verboom, and D. N. Reinhoudt, "Microring resonator based modulator made by direct photodefinition of an electro-optic polymer," Appl. Phys. Lett. **92**, 153310 (2008).
13. C.-T. Zheng, L.-J. Zhang, L.-C. Qv, L. Liang, C.-S. Ma, D.-M. Zhang, and Z.-C. Cui, "Nanosecond polymer Mach-Zehnder interferometer electro-optic modulator using optimized micro-strip line electrode," Opt. Quantum Electron. **45**, 279–293 (2012).
14. A. Leinse, M. B. J. Diemeer, A. Rousseau, and A. Driessen, "A novel high-speed polymeric EO Modulator

#308725 https://doi.org/10.1364/OE.25.031036
Journal © 2017 Received 6 Oct 2017; revised 10 Nov 2017; accepted 12 Nov 2017; published 28 Nov 2017

Optics EXPRESS

based on a combination of a microring resonator and an MZI," IEEE Photonics Technol. Lett. **17**, 2074–2076 (2005).
15. B. Bêche, "Integrated photonics devices on SU8 organic materials," Int. J. Phys. Sci. **5**, 612–618 (2010).
16. G.-M. Parsanasab, M. Moshkani, and A. Gharavi, "Femtosecond laser direct writing of single mode polymer micro ring laser with high stability and low pumping threshold," Opt. Express **23**(7), 8310–8316 (2015).
17. Y. Huang, G. T. Paloczi, J. K. S. Poon, and A. Yariv, "Demonstration of Flexible Freestanding All-Polymer Integrated Optical Ring Resonator Devices," Adv. Mater. **16**, 44–48 (2004).
18. Y. Huang, A. George, T. Paloczi, A. Yariv, C. Zhang, and L. R. Dalton, "Fabrication and Replication of Polymer Integrated Optical Devices Using Electron-Beam Lithography and Soft Lithography," (2004).
19. E. Nitiss, "Evaluation of performance of a hybrid electro-optic directional coupler and a Mach–Zehnder switch," J. Nanophotonics **11**, 16013 (2017).
20. H. Sato, H. Miura, F. Qiu, A. M. Spring, T. Kashino, T. Kikuchi, M. Ozawa, H. Nawata, K. Odoi, and S. Yokoyama, "Low driving voltage Mach-Zehnder interference modulator constructed from an electro-optic polymer on ultra-thin silicon with a broadband operation," Opt. Express **25**(2), 768–775 (2017).
21. R. Himmelhuber, O. D. Herrera, R. Voorakaranam, L. Li, A. M. Jones, R. A. Norwood, J. Luo, A. K.-Y. Jen, and N. Peyghambarian, "A Silicon-Polymer Hybrid Modulator—Design, Simulation and Proof of Principle," J. Lightwave Technol. **31**, 4067–4072 (2013).
22. F. Qiu, A. M. Spring, F. Yu, I. Aoki, A. Otomo, and S. Yokoyama, "Thin TiO2 core and electro-optic polymer cladding waveguide modulators," Appl. Phys. Lett. **102**, 233504 (2013).
23. N. Miyazaki, K. Ooizumi, T. Hara, M. Yamada, H. Nagata, and T. Sakane, "LiNbO3 optical intensity modulator packaged with monitor photodiode," IEEE Photonics Technol. Lett. **13**, 442–444 (2001).
24. R. C. Alferness, "Waveguide Electrooptic Modulators," IEEE Trans. Microw. Theory Tech. **30**, 1121–1137 (1982).
25. E. Dulkeith, F. Xia, L. Schares, W. M. J. Green, and Y. A. Vlasov, "Group index and group velocity dispersion in silicon-on-insulator photonic wires," Opt. Express **14**(9), 3853–3863 (2006).
26. C. Haffner, W. Heni, Y. Fedoryshyn, J. Niegemann, A. Melikyan, D. L. Elder, B. Baeuerle, Y. Salamin, A. Josten, U. Koch, C. Hoessbacher, F. Ducry, L. Juchli, A. Emboras, D. Hillerkuss, M. Kohl, L. R. Dalton, C. Hafner, and J. Leuthold, "All-plasmonic Mach–Zehnder modulator enabling optical high-speed communication at the microscale," Nat. Photonics **9**, 525–528 (2015).
27. A. S. Holland, A. Mitchell, V. S. Balkunje, M. W. Austin, and M. K. Raghunathan, "Fabrication of raised and inverted SU8 polymer waveguides," in H. Ming, X. Zhang, and M. Y. Chen, eds. (International Society for Optics and Photonics, 2005), p. 353.
28. M. Nordstrom, D. A. Zauner, A. Boisen, and J. Hubner, "Single-Mode Waveguides With SU-8 Polymer Core and Cladding for MOEMS Applications," J. Lightwave Technol. **25**, 1284–1289 (2007).
29. P. K. Tien, "Light waves in thin films and integrated optics," Appl. Opt. **10**(11), 2395–2413 (1971).
30. D. Marcuse, "Bending Losses of the Asymmetric Slab Waveguide," Bell Syst. Tech. J. **50**, 2551–2563 (1971).
31. K. Traskovskis, I. Mihailovs, A. Tokmakovs, V. Kokars, and M. Rutkis, "An improved molecular design of obtaining NLO active molecular glasses using triphenyl moieties as amorphous phase formation enhancers," in B. J. Eggleton, A. L. Gaeta, and N. G. Broderick, eds. (International Society for Optics and Photonics, 2012), Vol. 8434, p. 84341P.
32. A. Vembris, M. Rutkis, and E. Laizane, "Effect of corona poling and thermo cycling sequence on NLO properties of the guest-host system," Molecular Crystals Liquid Crystals **485**, 922684 (2008).
33. M. Rutkis, A. Vembris, V. Zauls, A. Tokmakovs, E. Fonavs, A. Jurgis, and V. Kampars, "Novel second-order non-linear optical polymer materials containing indandione derivativatives as a chromophore," in *Organic Optoelectronics and Photonics II*, P. L. Heremans, M. Muccini, and E. A. Meulenkamp, eds. (2006), Vol. 6192, p. 61922Q–61922Q–8.
34. E. Nitiss, E. Titavs, K. Kundzins, A. Dementjev, V. Gulbinas, and M. Rutkis, "Poling induced mass transport in thin polymer films," J. Phys. Chem. B **117**(9), 2812–2819 (2013).
35. J. L. Oudar and D. S. Chemla, "Hyperpolarizabilities of the nitroanilines and their relations to the excited state dipole moment," J. Chem. Phys. **66**, 2664–2668 (1977).
36. K. D. Singer, M. G. Kuzyk, and J. E. Sohn, "Second-order nonlinear-optical processes in orientationally ordered materials: relationship between molecular and macroscopic properties," J. Opt. Soc. Am. B **4**, 968–976 (1987).
37. K. Traskovskis, I. Mihailovs, A. Tokmakovs, A. Jurgis, V. Kokars, and M. Rutkis, "Triphenyl moieties as building blocks for obtaining molecular glasses with nonlinear optical activity," J. Mater. Chem. **22**, 11268–11276 (2012).
38. L. R. Dalton, "Rational design of organic electro-optic materials," J. Phys. Condens. Matter **15**, R897–R934 (2003).
39. P. K. Dey and P. Ganguly, "A technical report on fabrication of SU-8 optical waveguides," J. Opt. **43**, 79–83 (2014).

1. Introduction

For the last couple of decades, the development of new materials and waveguide structures for short-haul optical interconnects has been one of the hottest research topics in photonics research and industry. The central problem in this field is the realization of a high bandwidth

Optics EXPRESS

electro-optic (EO) modulator operating in the fJ/bit regime [1]. In this regard the use of organic EO materials has enabled the demonstration of unprecedented 0.7 fJ/bit EO efficiency in a silicon-organic device [2], over 170 GHz bandwidth in a plasmonic-organic devices [3,4] and sub-volt operation in an all-organic device [5], all operating in the infrared spectral range. The key to success of organic EO materials has been their multiple advantageous properties such as high EO coefficients reachable waveguide in devices [6–8], low optical absorption in the visible and infrared spectral range and compatibility with other commonly used inorganic and organic materials [9].

In this contribution we demonstrate an all-organic Mach-Zehnder interferometric (MZI) EO waveguide modulator comprising an SU-8 and a nonlinear optical (NLO) polymer operating in the visible spectral range near the first telecommunication window. The proposed all-organic waveguide EO modulator has been realized for the first time to author's knowledge. The employed SU-8 is an epoxy-based negative photoresist with low absorption coefficients in the visible and infrared spectral range, a high glass-transition temperature and good chemical durability. Also, low propagation loss <1.565 dB/cm in SU-8 waveguides can be achieved [10]. In our design SU-8 is used as the waveguide core and EO polymer is applied as a cladding. The proposed EO material is a glass forming polymer and used as a dopant in a low refractive index host. With such approach we were able to tune the optical and chemical properties of the cladding and avoid formation of crystallites. Possibility to tune the optical properties of the EO material is shown to be essential during device engineering step. The concept that SU-8 could be used as the host material for building all-organic integrated circuits follows from the observation that many effects such as EO switching [11–14], sensing [15] and lasing [16] have already been demonstrated in SU-8 based optical waveguide devices. Additional advantageous properties of SU-8 based optical waveguide photonics include wide spectral bandwidth and possibility to prepare devices on a mechanically flexible substrate which allows device shaping for specific purposes [17,18].

2. Modulator fabrication

2.1 Design and principles of operation

The all-organic MZI waveguide modulator design top-view and cross-section is illustrated in Fig. 1(A) and Fig. 1(B), respectively.

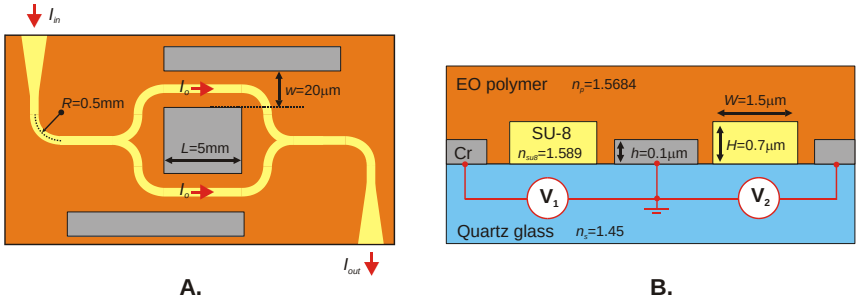

Fig. 1. A. The top-view and the dimensions of elements of the waveguide MZI, where I_{in} and I_{out} are the light input and output intensities, respectively; I_o – the light intensity in the MZI arm, R is the bend radius of the waveguide, w is the electrode separation length and L is the central electrode length. In the design the light input and output waveguides are purposely made to be far apart in order to avoid the scattered and uncoupled light reaching the detector at the output. B. The cross-section with dimensions of elements as well as refractive indexes at 633 nm of the waveguide MZI. The waveguide core is made of SU-8 and has the width W and the height H. The electrodes are made of Chromium (Cr) and have a height of h. Voltages V_1 and V_2 can be applied during poling and modulation.

The design has been profoundly described elsewhere [19]. It comprises an SU-8 waveguide core, electrodes in the plane with the waveguide core and an EO polymer coating.

Optics EXPRESS

A similar concept of having a thin passive waveguide core and an EO active cladding has been realized on Silicon-on-Insulator (SOI) platform as well as in a TiO_2 waveguide device only very recently [20–22].

The light output intensity I_{out} of the illustrated waveguide MZI depends on the phase difference of the beams in MZI arms. The I_{out} can be written as:

$$I_{out} = I_o\left(1+\cos\left(\varphi_o + \Delta\varphi\right)\right) \tag{1}$$

where I_o is the light intensity in each arm of the MZI, φ_o is the phase bias caused by the optical path length difference between the MZI arms, and $\Delta\varphi$ is the phase difference due to EO effect [23]. The last can be approximated by the equation:

$$\Delta\varphi = -\frac{k\cdot r\cdot n_g^3\cdot V\cdot L\cdot\Gamma}{2\cdot w}, \tag{2}$$

where k is the wavenumber, r is the effective EO coefficient, n_g is the group index in the waveguide, L is the interaction length, V is the applied voltage and Γ is the overlap integral between the applied electric field and the optical mode [24]. It is relevant to note the importance of using the group index n_g in Eq. (2). The n_g accounts for dispersion in the waveguide and should be calculated according to the equation [25]:

$$n_g = n_{eff} - \lambda\frac{dn_{eff}}{d\lambda}, \tag{3}$$

where n_{eff} is the effective refractive index. The group index and effective refractive index can differ significantly in waveguides where strong light confinement is present. Not accounting for group slowdown factor may lead to overestimation of EO coefficient [26]. Our calculations showed that in the proposed waveguide design the $n_g \approx n_{eff}$. This is because the waveguides are weakly confining the light and the material has low dispersion at the employed laser wavelength.

One of the most important parameters of an EO modulator is the drive voltage – voltage necessary to induce the phase variation $\Delta\varphi = \pi$. As evident from Eq. (2) the drive voltage can be reduced by increase of the modulator length L and by reduction of the inter-electrode distance w. Both result in an increased light propagation loss [8].

It is also important to have a high overlap integral Γ. For this in the design shown above it is favorable to have waveguides with modes less confined in the core. This results in the light to be more sensitive to the refractive index changes in the cladding. Higher Γ can be achieved by reducing either the size of the waveguide core or the contrast of the core and cladding refractive indices. Another favorable aspect of reducing the waveguide core dimensions and the core and cladding refractive index contrast is the possibility to have a single mode operation of the waveguide device [27,28]. However, mode penetration in the cladding may induce additional light propagation loss due to high interaction of light with the scattering boundary of the waveguide core [29] as well as due to radiation loss in the waveguide bends [30].

Despite the latter we aimed to make as small a waveguide core as possible for the sake of the highest EO efficiency. Our preliminary experiments showed that the smallest achievable SU-8 waveguides we can prepare with the available direct-write laser lithography have width W = 1.5 µm and height H = 0.7 µm. The waveguide core dimensions were fixed at the mentioned values. In the optimization step we concentrated on reaching the single transverse electric (TE) mode operation at 633 nm as well as increasing the overlap integral Γ by variation of the refractive index of the EO polymer.

Optics EXPRESS

2.2 EO polymer

We used a low molecular weight compound 2-(4-(bis(5,5,5-triphenylpentyl)amino)benzylidene)-1H-indene-1,3(2H)-dione (DMABI-Ph6) as an NLO chromophore for doping a PMMA matrix. DMABI-Ph6 is an organic glass forming compound with an absorption peak at 500 nm [31]. The absorbance spectrum and the molecular structure of DMABI-Ph6 is shown in Fig. 2(A). DMABI-Ph6 was selected mainly due to two reasons. Firstly, DMABI-Ph6 is amorphous and therefore would not crystallize during poling, unlike most of other DMABI derivatives [32]. Such effect is gained through attaching triphenylpentyl groups to the DMABI molecule. These groups limit the mobility of molecules which in turn reduces the probability of crystallization to occur. Crystallization of EO chromophores can cause lower EO efficiency, higher probability of dielectric breakdown and larger propagation loss. Secondly, the Maker fringe measurements performed at 1064 nm with a setup described elsewhere [33] done after corona poling [34] showed that DMABI-Ph6 possesses a high NLO coefficient – $d_{33}(532)$ = 69.2 pm/V. For this material the NLO coefficient values are resonantly enhanced due to the fact that the second harmonic of 1064 nm is in the absorption band. Therefore, to represent the optical nonlinearity of DMABI-Ph6 off optical resonance, we used the frequency corrected value according to [35] and got that $d_{33}(0)$ = 6.29 pm/V. By using EO and NLO coefficient relation from [36] we estimated that the EO coefficient r_{33} of DMABI-Ph6 at 633 nm should be around 3 pm/V. The EO material properties such as refractive index, glass transition temperature as well as EO efficiency are strongly dependent on the concentration C of DMABI-Ph6 in the PMMA matrix expressed as

$$C = \frac{m_{DMABI-Ph6}}{m_{DMABI-Ph6} + m_{PMMA}}, \tag{4}$$

where $m_{DMABI\text{-}Ph6}$ is the mass of the chromophore and m_{PMMA} is the mass of PMMA. Below in Fig. 2(B) the measured glass transition temperatures as well as the NLO coefficients at zero frequency are shown as functions of DMABI-6Ph mass concentration C. The glass transition temperature T_g was estimated from the second harmonic generation intensity decay measurements as described elsewhere [37]. As evident the T_g drops and saturates to around 77 °C at as little as 10% mass concentration (wt) of DMABI-Ph6 in PMMA matrix. On the secondary axis of Fig. 2(B), we plotted the measured NLO coefficient $d_{33}(0)$ which increased in the second order with the increase of chromophore concentration. This was surprising because a drop in the optical nonlinearity was being expected at higher chromophore number density due to dipole-dipole interaction [38].

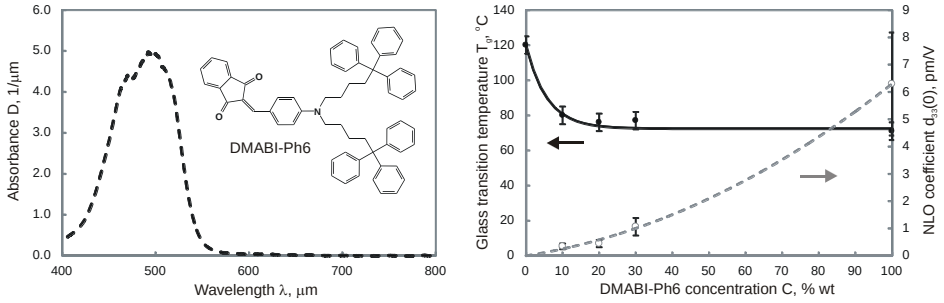

Fig. 2. A. An absorbance spectrum as well as the molecular structure of nonlinear optical chromophore 2-(4-(bis(5,5,5-triphenylpentyl)amino)benzylidene)-1H-indene-1,3(2H)-dione (DMABI-Ph6). Absorbance was measured for a 300 nm thick DMABI-Ph6 film on a quartz glass substrate. B. The glass transition temperature (black line plotted against the primary y axis) and the NLO coefficient at zero frequency (grey line plotted against the secondary y axis) as a function of DMABI-Ph6 concentration in PMMA.

Optics EXPRESS

Below in Fig. 3 the effective refractive indexes n_{eff} of the first two modes and the corresponding overlap integral Γ of the first mode at 633 nm in the waveguide as a function of DMABI-Ph6 chromophore concentration has been depicted. There the secondary x axis also indicates the refractive index of EO polymer measured using a commercial prism-coupler Model 2010 (Metricon). The n_{eff} and Γ were calculated using finite element mode solver in Comsol Multiphysics 5.2a Wave Optics module.

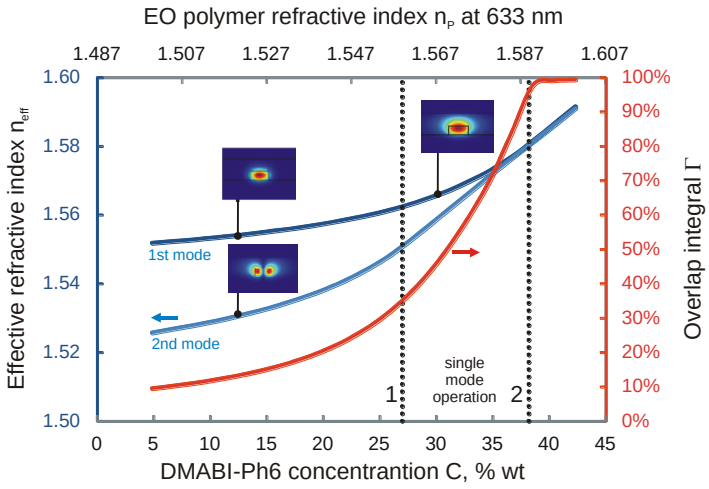

Fig. 3. The blue lines plotted on primary y axis indicate the effective refractive index n_{eff} of first and second TE modes as a function of DMABI-Ph6 concentration in PMMA matrix, while the red line plotted on secondary y axis indicates the overlap integral Γ of the 1st mode. The first dotted vertical line indicates concentration threshold above which the waveguide operates in single mode regime. The second dotted vertical line indicates the concentration at which the EO polymer becomes the waveguide core. The secondary x axis shows the corresponding refractive index n_p of EO material.

As evident from Fig. 3 the effective refractive indices of 1st and 2nd TE modes increase with DMABI-Ph6 concentration. At around 27% wt threshold indicated by the dotted line 1 in Fig. 3, the second mode is almost entirely in the cladding and single mode operation of the waveguide is achieved. Further increase of concentration will result in EO polymer refractive index above that of SU-8. The refractive index n_{SU8} of SU-8 after hard-bake was measured to be 1.589. This threshold is indicated by the vertical dotted line 2 located at 38% wt. The line indicates the concentration C above which the EO polymer would become the waveguide core and guiding through the waveguide MZI would be impossible. The waveguide device should be prepared with the DMABI-Ph6 concentration between 27 and 38% wt which results in overlap integral Γ to be in the range from around 30 to 90%. It is again important to emphasize that the bend loss of guided mode increases dramatically with the reduction of the refractive index contrast between the waveguide core and cladding [30]. In order to reduce the light propagation loss, it was decided to employ EO polymer with the DMABI-Ph6 concentration in PMMA matrix of 30% wt resulting in overlap integral Γ of around 50% and the estimated EO coefficient r_{33} of around 0.65 pm/V.

2.3 Fabrication steps

The device was fabricated on a 1 mm thick quartz glass substrate with refractive index n_s of 1.45 (Quartz Scientific). The quartz glass was preferred to soda lime due to its higher resistivity. Preliminary investigations of polymer poling with lateral electrodes were also performed on soda lime glass. After poling morphology changes in electrodes were found to have taken place. X-ray photoelectron spectroscopy (XPS) measurements showed that morphology changes were due to Sodium (Na) diffusing out of the glass while Cr diffusing

Optics EXPRESS

inward. Such occurrence caused severe increase of light propagation loss due to scattering on the electrode boundary. The effect was not observed when poling was done on quartz glass substrates.

The quartz glass substrate was cleaned in a piranha solution H_2SO_4 + H_2O_2 1:10 for 10 min followed by a DI water and isopropanol rinse. After substrate cleaning a positive resist MEGAPOSIT SPR 700 was spin-coated on the substrate followed by an electrode mask exposure using a 365 nm laser writer µPG 101 (Heidelberg Instruments). Then AUTO 306 thermal evaporator (Edwards) was used to sputter 100 nm thick Cr electrodes. The electrode separation w was 20 µm while the central electrode length L was 5 mm. The SU-8 resist was prepared from GM-1075 (Gerseltec) by diluting it in gamma-Butyrolactone in mass proportion 1:1. After removal of positive resist, a 0.7 µm thick SU-8 layer was spin-coated on the sample at 4000 rpm/s. Then the MZI waveguide structure was exposed using µPG 101, developed in mr-Dev 600 (Micro Resist Technology) and rinsed in isopropanol. The MZI was made with waveguide bends of R = 500 µm and one of the MZI arms longer so that the phase bias would be $\varphi_o = \pi/2$. The resist was hard-baked on a hot-plate at 160 °C for one hour. On top of the structure, a 1 µm thick EO polymer DMABI-Ph6 + PMMA 30% wt film was spin-coated from a chloroform solution. The electrical wires were connected to Cr electrodes by Silver (Ag) paste. Poling was done on a temperature stabilized hot-plate by setting the poling voltage with a 6517B electrometer (Keithley). The poling setup was computer controlled and allowed monitoring of poling temperature as well as currents in time. Preliminary experiments showed that dielectric breakdown occurs during the poling if poling temperature is above 101 °C and poling voltage is above 900 V. Therefore the EO polymer in the device was poled slightly below this threshold – at 96 °C and the poling voltage of $V_1 = V_2 = 800$ V for 15 minutes. The poling temperature was thus around 20 °C above T_g. The lower side of the substrate was then slightly cut using a diamond saw thus allowing fine breaking of the substrate and the waveguides. The light could be coupled into the waveguide through the facet without any additional polishing or preparation steps with low insertion loss as also demonstrated elsewhere [39].

3. Experimental setup and measurements

Below in Fig. 4 the optical images (A and C) as well as the setup used for electro-optic characterization of the device (B) has been illustrated. In the setup we used a 2 mW He-Ne laser operating at 633 nm as light source which was positioned such that TE mode in the waveguide would be excited. The laser beam was coupled to the MZI and collected via 20x microscope objectives. We used a function generator, phase inverter and a dual-channel amplifier PZD350 (Trek) to apply the modulating voltage in a push-pull regime. The central electrode was kept to ground while square signals with opposite phases were applied to the side electrodes. The light intensity modulations were recorded using a silicon (Si) photodetector connected to an oscilloscope. In Fig. 4(C) a top-view optical image of waveguide MZI with excited guiding mode is shown. As mentioned above the waveguide MZI is purposely made asymmetric with a phase bias of $\varphi_o = \pi/2$. This results in part of the energy to be scattered in the form of radiation modes at the second waveguide splitter due to destructive interference. Unfortunately, this scattering is weakly pronounced in the Fig. 4(C) due to poor dynamic range of the camera.

Optics EXPRESS

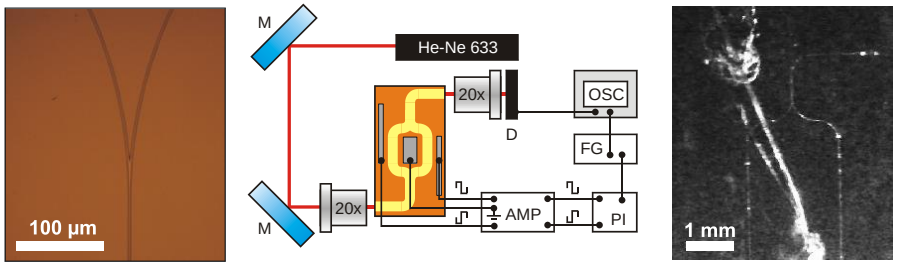

Fig. 4. A. An optical image of SU-8 waveguide splitter. B. The setup for electro-optic characterization of the device: He-Ne 633 – laser, M – mirrors, D – detector DET36A (Thorlabs), OSC – oscilloscope, FG – function generator, PI – phase inverter, and AMP – amplifier. C. An optical image of the waveguide MZI with excited guiding mode.

The output light intensity I_{out} as well as the applied modulating field intensity E in time is displayed in Fig. 5. As evident from the graph the modulation bandwidth is very low – at around 4 kHz. The main reason for this is the poor electrical connection between the modulator electrodes and wires. The measured contact resistance of the Ag paste connected wires was around 1 kOhm, while the capacitance of wires in the electrical circuit including those of testing equipment was measured to be around 0.2 nF. The combination of both give the theoretical modulation bandwidth limit of around couple of kHz due to the RC time constant which has good agreement with the observations. In theory the capacitance of the modulator should be very low due to a small overlap area of the electrodes and a low dielectric constant of the EO polymer.

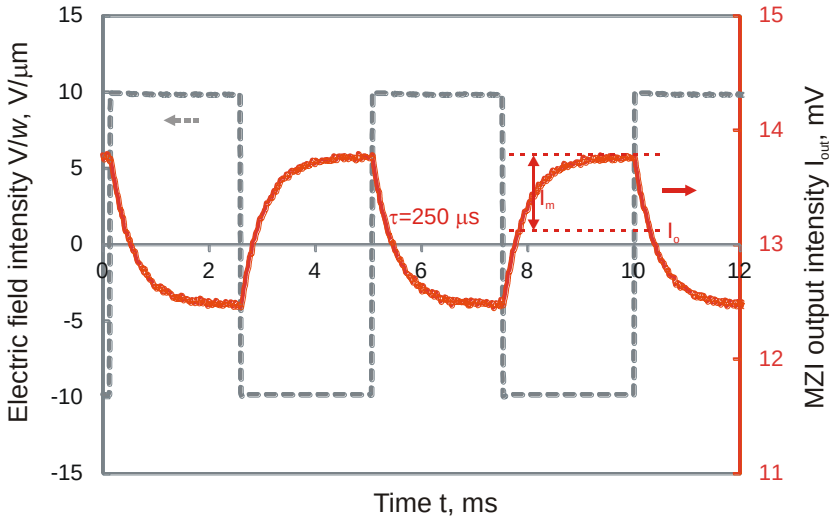

Fig. 5. The applied modulating field intensity V/w (the grey line plotted against the primary y axis) and the output light intensity I_{out} (the red line plotted against the secondary y axis) as a function of time.

For estimating EO coefficient from the obtained modulation data displayed in Fig. 5 we first use an approximation:

$$I_m = \frac{dI_{out}}{d\varphi}\Delta\varphi. \tag{5}$$

Optics EXPRESS

By setting the bias point $\varphi_o = \pi/2$, from (5) we get that the modulated phase amplitude $\Delta\varphi$ is the ratio of modulated signal amplitude I_m and the MZI output intensity $I_{out} = I_o$ at $\varphi_o = \pi/2$. After combining Eq. (2) and Eq. (5), we get

$$r = \frac{I_m}{I_o} \frac{\lambda \cdot w}{\pi \cdot n_g^3 \cdot V \cdot L \cdot \Gamma}. \quad (6)$$

By using (6) we find the EO coefficient r = 0.20 pm/V. This is approximately 30% of the value estimated from the NLO measurement in thin films which is close to typically achieved values demonstrated in literature [8].

Obviously the efficiency of the device is very poor mainly due to low optical nonlinearity of used EO polymer. The main reason for this is clearly the fact that the device is probed with wavelength that is far from the optical resonance. By the cost of increased light absorption one could probe the device with a wavelength near resonance which would result in truly enhanced observable EO efficiency in the same material. It is recognized that the EO modulator should have the drive voltage of no more than the TTL level of 5 V for it to have a widespread commercial utilization [9]. By using Eq. (2) we estimate that this threshold for the demonstrated device could be achieved if the EO coefficient of polymer cladding would exceed 130 pm/V which can be gained in the current state-of-the-art organic EO materials [7].

4. Summary

We have demonstrated a novel all-organic EO modulator operating in the visible wavelength range. The preparation employs two optical lithography steps where the first step is used for defining the electrode pattern and the second – for defining the waveguide core in SU-8 photoresist. Optical nonlinearity is achieved by introducing a novel host-guest EO polymer as waveguide cladding. The employed glass forming EO material allows broad tuning of refractive index. The EO chromophore concentration at which the waveguide operates in single-mode regime was found during by numerical optimization of device. The waveguides were prepared on a quartz glass substrate. Quartz glass were preferred over to soda lime because of higher resistivity which prohibited ion diffusion and electrode destruction during in-plane polymer poling. From the experimental EO modulation data we find that the poled polymer has the EO coefficient of 0.2 pm/V which is around 30% of the value estimated from the NLO measurement in thin films.

Funding

Institute of Solid State Physics, University of Latvia (SJZ/2016/26); Ministry of Education and Science, Republic of Latvia (MultIfunctional Materials and composItes, photonicS and nanotechnology (IMIS2)).

Acknowledgment

We acknowledge Dr. Anatolijs Sarakovskis at Institute of Solid State Physics for the XPS measurements.

Institute of Solid State Physics, University of Latvia as the Center of Excellence has received funding from the European Union's Horizon 2020 Framework Programme H2020-WIDESPREAD-01-2016-2017-TeamingPhase2 under grant agreement No. 739508, project CAMART²